Equilibrium dynamics of single DNA molecules confined to nanopit structures

Hugo B. Brandao*[1], Walter Reisner[2]

[1,2]Department of Physics, McGill University, 3600 rue University, Montreal, Quebec, Canada H3A 2T8

ABSTRACT

Introduction: Of great interest in the physical sciences today, is the study of single molecules in nano-fluidic devices. These 'labs-on-a-chip' can provide the basic framework for quantifying the behavior of molecules, such as polymers, under confinement. This study is an investigation of a theoretical free-energy model used to predict thermodynamic properties of DNA molecules situated in a device called a nanopit array. Two parameters in the model, molecule length and nanopit width, are varied and tested against experimental data. **Methods**: Video-fluorescence microscopy was used to image single DNA molecules in the nanopit array; analysis consisted of determining the average number of nanopits occupied by a single DNA molecule over time. **Results**: Good qualitative agreement was reached between theory and experiment for the nanopit width variation, but molecule-length variation predictions were shown to still need improvement. A least-squares fit of the theory to the data suggested that the entropic parameter, A, and the excluded volume term, B, have a modified dependence on nanoslit height and nanopit depth than what is currently predicted by the model. **Discussion**: These experiments confirm that the theoretical model is adequate under certain regimes and predicts conditions under which theory and experiment may significantly diverge. Modifications to the theory are proposed.

KEYWORDS

DNA, nanopit array, fluorescence video-microscopy

*Corresponding author:
hugo.brandao@mail.mcgill.ca

Received: 2 January 2011
Revised: 13 March 2011

INTRODUCTION

Serious theoretical treatment of the fundamental behaviour of polymers began in the late 1960's and early 1970's with some groundbreaking scaling arguments by de Gennes *(1)* and Edwards *(2)*. It has only been in recent years *(3)*, with the advances in nano/microfabrication techniques, that emerging nano-fluidic devices such as nanopores, nanochannels, and nanoslits have been able to rigorously test some of these early theoretical models *(1,2)*.

Recent experiments have probed the effects of geometric confinement on individual DNA molecules in one-dimensional nanochannels *(3,4)* and in two dimensional nanoslits *(5,6)*. When the walls of the nano-fluidic device confine the DNA below its bulk characteristic size in solution (i.e. the radius of gyration), both the static and dynamic behaviour *(6)* of individual molecules is altered due to the steric interactions of the DNA with its confining walls, as well as the hydrodynamic self-interactions.

This study is a further exploration of a new kind of nano-fluidic device, the nanopit array, developed initially by Reisner *et al. (7)* in 2008. Nanopit arrays are nanoslits, which consist of a thin slit between two wafers with a lattice of embedded nanopits on the bottom wafer, as seen in Fig. 1. A DNA molecule confined to a nanopit will assume a stable configuration that minimizes its free-energy. In its search for a state of equilibrium, a given DNA molecule will either fill a single nanopit or span multiple nanopits depending on its contour length *L* and geometric parameters such as slit height *h*, pit depth *d*, pit width *a*, and pit spacing *l*. When a molecule spans multiple pits, the amount of molecule in a given pit fluctuates in time as molecules exchange contour back and forth due to Brownian fluctuations *(7)*.

From a technological point of view, nanopit arrays provide a simple way to manipulate single DNA molecules on a chip, providing more flexibility and precision than conventional nanoslits, and more degrees of freedom than nanochannels. For example, it is possible to imagine - using nanopit arrays in conjunction with embedded nanopores in each pit - that one could perform highly localized chemistry on a particular appealing segment of DNA or some generic polymer. Furthermore, nanopits may be useful in applications such as single-molecule denaturation mapping in nano-fluidic channels *(8)*. For instance, if nanopits were etched into a nanochannel, they might serve as local reservoirs for temporarily unneeded molecule segments, while the segments of DNA undergoing analysis extend into the nanochannel. Once a given segment has been analysed, pressure can be applied to drive contour from the reservoir into the nanochannel and to shift the analysed contour segment into an adjacent reservoir.

The aim of this paper is to test the free-energy model presented by Reisner *et al. (7)*. With this model, it is possible to predict thermodynamic quantities from a chip's geometry and DNA molecule properties. By separately varying the DNA molecule's length *(L)* and nanopit width *(a)*, experimental data was gathered using fluorescence video-microscopy of single λ-DNA molecules in the nanopit arrays; the data was analyzed using the numerical programming package, MATLAB.

The viral DNA molecule (λ-DNA) was used in this experiment to allow for experimental comparison to previous work done by Reisner *(7)* and to extend his previous work. Measurements of the average number of nanopits occupied by a molecule versus pit width were carried out for a width range of 250-1000nm and compared to the model's predictions. A similar analysis was performed for molecule-length variation using a λ-DNA digest. The integrated intensity of each fragment was used to determine molecule length and a plot of the average nanopit occupancy versus molecule size was made. Using this method, occupancy probabilities were tested against the theoretical predictions for two different parameters in the current model.

BACKGROUND

THEORY FOR OCCUPANCY STATISTICS

Consider a DNA molecule of length *L* constrained to occupy *N* nanopits in a 2D lattice. Next, assume that each pit contains an equal amount of DNA. A molecule can arrange itself in several different ways on the lattice depending on the number *N*; the upper and lower bounds of *N* are set by the physical limitations of its stretching and compressing within the nanopit lattice.

Now, as a consequence of the discrete number of occupied nanopits, the number of energy states accessible to a molecule is effectively quantized. For a particular geometry, the molecule will favour arrangements in a certain number of N nanopits more than others. Provided a model *(7)* to quantify the free energy (ΔF_{tot}) of a molecule within the nanopit array as a function of *N*, the probability, P_N, that *N* pits are occupied can be calculated from

$$P_N = \frac{\Omega_N e^{\frac{-Ftot(N)}{k_B T}}}{\sum_N \Omega_N e^{\frac{-Ftot(N)}{k_B T}}} \qquad [1]$$

Ω_N, the degeneracy, is the total number of different ways of assembling a molecule, in a self-avoiding manner, on a square lattice with *N* occupied pits; it represents the number of states with the same energy. Values for Ω_N can be found in literature *(9)* for N=1 up to N=28. k_B and *T* are Boltzmann's constant and temperature respectively.

The molecule's dynamics should be Brownian in the absence of external sources of fluid flow such as applied electric fields or pressure gradients *(10)*. Hence, it can be rationalized that since adjacent nanopits are identical, each pit contains approximately an equal amount of DNA. Thus, the total contour length *L* can be subdivided into the amount of contour within each pit (L_p), and the amount in the nano-slit, in between the pits, (L_s) to obtain

$$L = N L_p + (N-1) L_s \qquad [2]$$

The change in free energy from *(7)* is then given by

$$\Delta F_{tot} = N\left(F_p - F_s\right) + \left(N-1\right) F_{spring} \qquad [3]$$

(F_p - F_s) is the difference free energy of contour L_p placed in a nanopit versus in a nanoslit, and F_{spring} is an energy term

accounting for the free-energy required to stretch the DNA molecule between nanopits. From a series of polymer theory scaling arguments, F_p - F_s can be re-written as

$$F_p - F_s = -AL_p + BL_p^2 \qquad [4]$$

The parameters *A* and *B* depend on the geometric restrictions of the nanopit array *h*, *d*, *a*, (Fig. 2A) and properties of the DNA molecule, including its persistence length P (the minimum length-scale for which a segment of DNA cannot self-interact) and the width of the molecule *w*. The spring energy *(7)* is given by,

$$\Delta F_{spring} = \frac{l^2}{2PL_s}\left(1 + \frac{1}{2(1 - l/L_s)}\right) \qquad [5]$$

Minimization of the free energy in Eq.3 after the appropriate substitutions of equations 2, 4, and 5, yields the equilibrium value of L_p. Substitution of this value back into Eq.3 determines the equilibrium free energy; curves for the occupancy probability can then be generated by varying one parameter (such as *L* or *a*). Finally, the average pit occupancy for a molecule will be given by

$$n_{avg} = \sum_N N \cdot P_N \qquad [6]$$

EXPERIMENTAL METHODS

EXPERIMENTAL PROCEDURE

Data was collected for fluorescence video-microscopy using a Nikon Eclipse Ti-U inverted microscope equipped with an Andor iXON camera capable of single-photon detection and a 100× 1.4 N.A. oil-immersion objective lens. Nanopit depth and slit height of sample nanopit arrays were measured to be 71±2 nm and 69±2 nm respectively with a profilometer. SEM micrographs of the nano-fluidic chip reveal the pit widths to be 250nm, 300nm, 350nm, 400nm, 500nm, 600nm and 1000nm. These measurements had a 4.4% fractional error at the 95% confidence level as determined from image analysis of the SEM micrographs. Spacing in between pits was fixed at 1 μm for all experiments conducted. Figures 2B and 2C show sample scanning electron microscope (SEM) images of an array of nanopits consisting of 1 μm pit-to-pit spacing and 300nm pit width in typical square lattice geometry.

A silica nano-fluidic chip containing a series of nanopit arrays of varying geometry was held on a chuck by an aluminum retaining ring. Application of pneumatic pressure to run the DNA from the loading reservoirs into the nanopit arrays was ensured by the O-ring seals. Figure 3 shows a schematic diagram of the experimental setup.

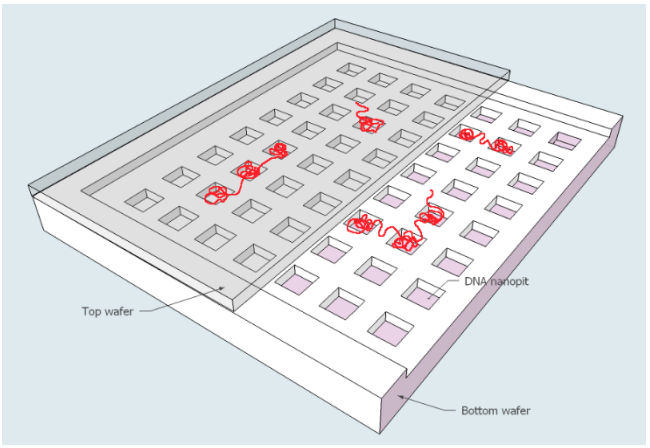

Fig. 1. Three-dimensional schematic diagram of nanopit array. In red is a representation of DNA molecules in the nanopits. The nanopit arrays were constructed on fused silica wafers using a combination of electron beam and UV contact lithography.

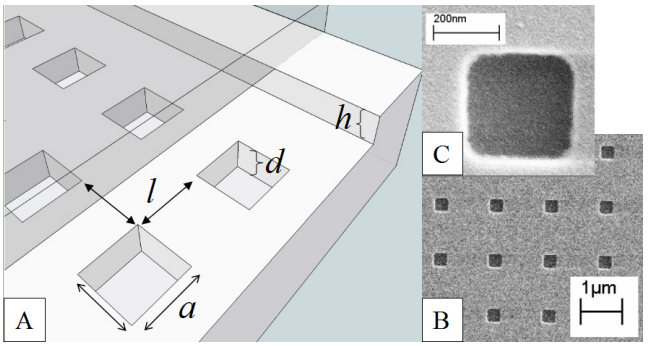

Fig. 2. Close-up view of nanopits in a chip. A) Outline of the important geometric parameters required in the theory to predict DNA occupancy states: slit height (*h*), pit width (*a*), pit depth (*d*), and pit spacing (*l*). B,C) SEM micrograph of an array of nanopits with 1μm pit-to-pit spacing and 300nm pit width.

The DNA was suspended in 10 mM Tris buffer measured at a pH of 7.92±0.02 and a conductivity of 0.53±0.02 mS. The experiment was run using λ-phage DNA (48.5kbp) from New England BioLabs stained with YOYO-1 fluorescent dye (Invitrogen) with a DNA base pair to dye concentration of 5:1. Due to the staining process, the length of the DNA molecule was estimated to increase from 16.5μm to 21μm as was measured by Reisner *et al.* in 2007 *(4)*. To repress photobleaching of the dye and photo-knicking, β-mercaptoethanol was added to the buffer to create a 2% volume/volume solution.

Before conducting the experiment, both the buffer solution and a buffer-filled chip containing the nanopit arrays were left to de-gas overnight. Thus, flow-inducing air bubbles in the microchannels of the chip were effectively removed. Approximately 20μl of the

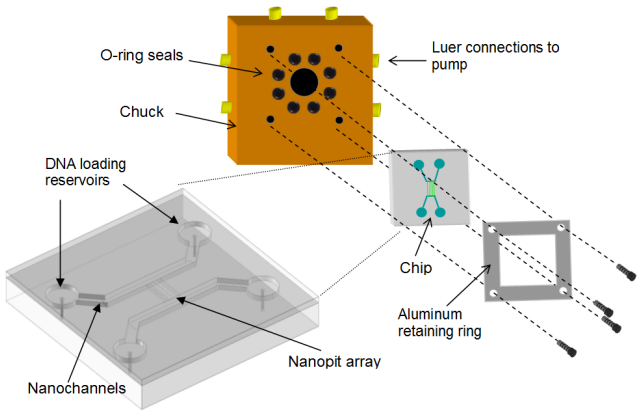

Fig 3. Schematic diagram of chuck and chip. DNA is loaded into the circular loading reservoirs using a micropipette and run with pneumatic pressure ensured via o-ring seals. Small bursts of pressure can be applied to drive DNA from the nanochannel into the nanopit arrays to be imaged. Diagram reproduced but modified from (4) with permission by the author.

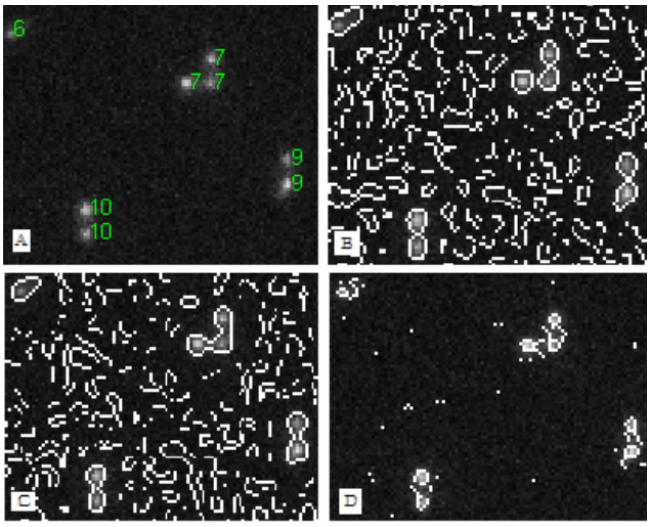

Fig 4. Comparison of various edge-detection techniques available for image analysis. A) Unprocessed fluorescence video-microscopy image taken of λ-DNA molecules; exposure time is 0.1s. B) Edges found via the Laplacian of Gaussian method using an unprocessed image. C) Edges found via the Laplacian of Gaussian method using processed images averaged over three frames. D) Edges found via the Sobel edge-detection method.

prepared DNA/buffer solution was manually loaded the next day with a micropipette into each of the four reservoirs on the chip. 100-200 mbar of pneumatic pressure was used to drive DNA from the reservoirs into the nanoslit to avoid fragmentation of the molecules. Short bursts of 1000-1500 mbar of pressure were then applied to each of the four reservoirs individually to equalize the fluid levels and to minimize unwanted flow. Molecules were allowed to relax in the nanopits for 30-40 seconds after being driven into the nanoslit. Data was acquired continuously by the CCD camera with 100-200 ms exposure times, in frame transfer mode, with negligible delay between image acquisitions. Experiments were conducted at room temperature.

DATA ANALYSIS

Images of the DNA molecules were analysed using MATLAB. A rectangular lattice of square boxes was aligned to the nanopits by the user via a graphical user interface. Occupancy of a nanopit was then established by determining the average pixel intensity value within each box; if the mean intensity within a box was above a certain threshold, then the pit was deemed filled. The threshold parameter was adjusted manually for each image sequence; this flexibility allowed the user to chose the most appropriate value for a given experimental condition and quality of image. Figure 4A shows a typical video-microscopy image of the DNA molecules in the nanopit arrays. Occupied nanopits have all been identified and each nanopit is registered to a particular molecule (indicated by the numbering of each pit).

To distinguish between two molecules in adjacent nanopits, the program relied on an edge-detecting function available in the MATLAB library. This function worked by applying a Gaussian filter to the image via standard convolution methods and a Laplacian operator to detect areas of rapid intensity changes. The algorithm would output an image with the boundary of a molecule clearly defined. If two adjacent nanopits were enclosed by such a boundary, then a single molecule occupied both pits; otherwise, the pits were occupied by different molecules.

The Laplacian of Gaussian method of edge detection performed very well locally. Due to its local nature, it quickly enhanced noise as is evident in figures 4B and 4C; nevertheless, it remained the preferred method of edge detection. Other edge-finding methods were considered including the Roberts and Sobel methods *(11)*. While they often found the DNA molecule edges and did not enhance noise, they failed to produce a smooth, *closed* contour of the whole molecule as can be seen in comparing figure 4D to figure 4B and 4C.

An issue inherent in the short exposure times of 100 ms (used to acquire a detailed profile of the pit-to-pit contour fluctuations of a molecule) was that molecule segments in between pits occasionally disappeared from certain frames. For instance, the bottom left nanopit occupied by molecule 7 in figure 4B appeared disconnected from the other two pits. However, inspection of a sequence of images revealed that all three nanopits belonged to the same molecule.

An approach that proved to be very effective to remedy this kind of problem was to perform image averaging: Each image from the video was averaged with the image in the frame before and

after it before undergoing analysis by the edge-detection algorithm. As an example of the effectiveness of this technique, compare molecule 7 in figure 4B to figure 4C: the link that was previously not apparent has been intensified and picked up by the Laplacian of Gaussian edge-detection algorithm.

To justify the use of frame-averaging, we investigated the timescale for the contour fluctuation of a molecule in between two nanopits: averaging was warranted as long as the time-scale was below the correlation time of pit-to-pit contour fluctuations. By integrating the pixel intensities of each nanopit registered to a series of user-defined boxes, the fluorescence of each pit was found. Then, the correlation coefficient was computed at a series of time lags using the GARCH model (11) for the cross-correlation of integrated intensity between two adjacent pits.

The cross-correlation plots for the integrated intensity of each nanopit were used to determine that, at 95% confidence, it takes between five to ten frames (0.5-1.0s) for contour fluctuations to become uncorrelated. What this signifies is that it takes 5-10 frames for the contour segment in one pit to have no memory of a significant fluctuation that occurred in the adjacent pit. Our frame-averaging combined images for 0.3s, which is 40% less than the smallest observed correlation time, suggesting that we can use frame-averaging without much worry. Figure 5 shows a sample of this result.

RESULTS AND DISCUSSION

JUSTIFICATION OF THE ASSUMPTION OF EQUAL CONTOUR PER NANOPIT

In Section II, the quantization of the energy states of a molecule was introduced by assuming equal amount of molecule per nanopit. This theoretical assumption was initially justified by claiming that all the nanopits were identical; thus, a DNA molecule should fill all nanopits equally. Experimental analysis of seven randomly selected molecules shows that for time intervals taken at least ten times greater than the average correlation times for pit-to-pit fluctuations, nanopits do indeed contain an equal amount of contour to within 4%. The percentage error between the mean pit intensity (within a single user-defined box, i) and the averaged mean intensity for all nanopits occupied by a molecule was computed by:

$$\%\,\text{error}(i) = \frac{X_i - \overline{X}}{\overline{X}} \times 100\% \qquad [7]$$

X_i is the mean intensity of nanopit i and $\overline{X} = \sum_{i=1}^{N} X_i / N$ is the averaged mean intensity.

VARIATION OF MOLECULE LENGTH

It is known that molecule intensity should vary linearly with contour length if the DNA is uniformly stained with an appropriate dye *(8)*. Consequently, when analysing the video-microscopy images for a λ-(mono) DNA digest (New England BioLabs), it was possible to estimate the length of each fragment by using a simple ratio. The nanopit array geometry under analysis consisted of 1 μm pit-to-pit spacing, 100 nm pit depth and slit height, and 300 nm pit width. The experimental fluorescence video-microscopy images were collected by Reisner at the Technical University of Denmark and were processed and analysed with his permission.

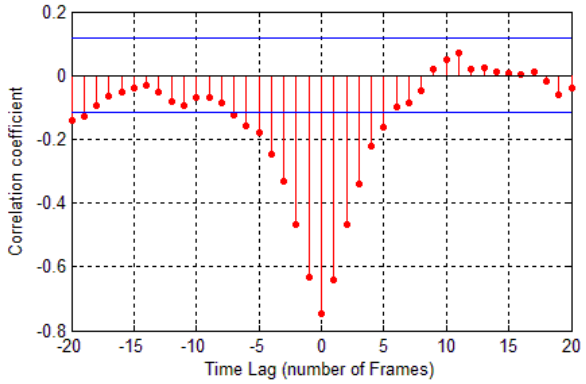

Fig 5. Sample cross-correlation plot of pit-to-pit contour fluctuations of a DNA molecule in a nanopit array with geometry l=1μm, a=300nm, h=d=100nm. Correlation coefficients within the horizontal blue bars delimit uncorrelated data to within a 95% confidence level.

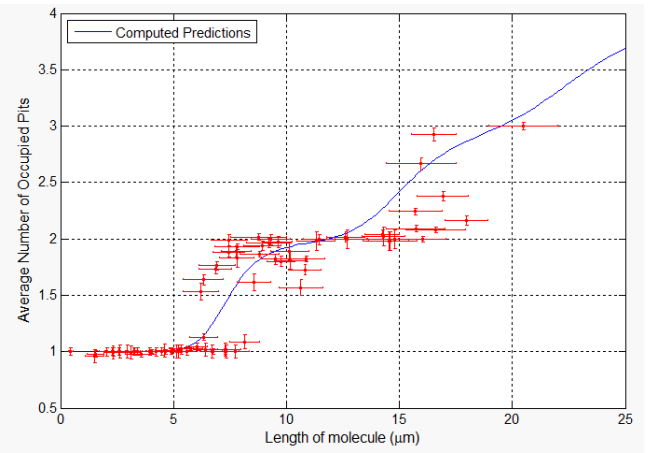

Fig 6. Average nanopit occupancy of a digest of λ-DNA fragments in a nanopit array of dimensions a=300nm, h=d=100nm, l=1μm. Error bars are reported for both the intensity and occupancy at 68% confidence. The solid line is the theoretical prediction for n_{avg} as a function of contour length.

The ratio of pixel intensity to contour length was calibrated using values from previous experiments *(7)*, where it is shown that a full-length λ-DNA molecule occupies on average 3.2±0.1 nanopits. In this experiment, the molecule exhibiting the greatest average occupancy state for the DNA digest (n_{avg} = 3.01±0.05) was taken to be 21 μm long. The two results are not comparable within error; however, for the purposes of qualitative comparison of the data to the theory, the difference is small enough to ignore.

Average pit occupancy was plotted against contour length for 82 different molecules together with the theoretical predictions. The theoretical curve was obtained from using the values for the persistence length *P*, chain thickness w, and geometric parameters of the chip used by Reisner *et al.* in the 2008 study *(7)*. As observed in figure 6, the average occupancy varies very non-linearly with contour length in what appears to be a series of steps. While the theoretical curve seems to follow the general trend of the molecule's distribution, it seems to first underestimate then overestimate the average occupancy at the transitions between n_{avg} states occurring at *L*=7.5 μm and *L*=17 μm respectively. Moreover, the average nanopit occupancy at around 17μm increases very suddenly from n_{avg}=2 to n_{avg}=3. This sharp transition in the experimental data is not evident in the theoretical computation, where instead shows a smooth curve extending from 10 μm to 20 μm. The error bars in figure 6 are computed from the standard deviations of the integrated intensity and average occupancy.

To accommodate a quantitative discussion for length-variation analysis would require that we be able to discriminate clearly between the different fragment sizes in the DNA digest. The λ-mono DNA digest from New England BioLabs contains seven distinct fragment sizes for DNA. We can make histograms of the average occupancy versus contour length and look for areas where the contour length peaks. These peaks should occur at the contour-length values of the fragment sizes in the digest. Figure 7 displays a result of a histogram done for the points of figure 6. For instance, the peak at around *L*≈14.5 μm in figure 7 clearly corresponds to the molecule fragment of length 33,498 base pairs; many of the other fragment lengths can be identified in this way.

With more data points, a Gaussian fit to the binned data can give a better idea of the scatter of each fragment size, and will allow us to better estimate the average occupancy error for various different molecule lengths. To reduce the error in the experiments due to white noise, it is possible to subtract the average background from the image before pixel integration; besides increasing the signal to noise ratio, this further ensures that results from different experiments can be compiled together, without offset due to different experimental conditions.

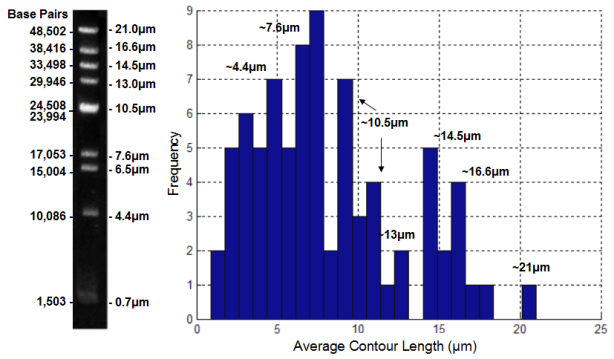

Fig 7. Histogram of the experimental data for the average contour length of a molecule. Peaks distinctly correspond to the fragment sizes observed for the agarose-gel electrophoresis results of a λ-mono DNA digest. Gel-electrophoresis © image reproduced by permission from New England BioLabs.

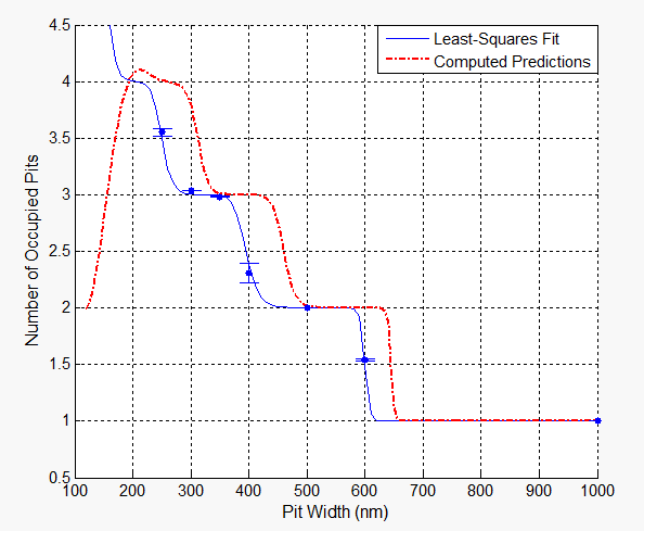

Fig 8. Least-squares-fit of data to theory and comparison to the predicted results obtained from the current definitions of parameters A_o and B_o. Error bars on the data points are the standard error on the averaged mean occupancy for 4, 15, 18, 4, 27, 35 and 21 molecules corresponding to pit widths 250nm, 300nm, 350nm, 400nm, 500nm, 600nm and 1000nm respectively.

C. VARIATION OF PIT WIDTH

An experiment was conducted for L fixed at 21 μm, *h*=*d*=70nm, l=1 μm. A total of 124 molecules were analysed for the average nanopit occupancy with respect to nanopit width. The results were plotted with their associated errors in figure 8. To generate the least-squares-fit curve the following error function was minimized by varying parameters A_o and B_o.

$$\chi = \sum_{a} \left(n_{avg}(A_o, B_o) - n_{exp} \right)^2 \qquad [8]$$

The value of n_{avg} is the numerical result for the mean pit occupancy of a molecule and n_{exp} is the experimentally measured average. In the current theory there are two parameters *A* and *B* which account for the nanopit free energy. The cited scaling (7) of these parameters is

$$A \sim P\left(\frac{1}{h^2} - \frac{1}{(h+d)^2} - \frac{2}{a^2}\right) \quad [9]$$

$$B \sim \frac{w}{(h+d)\ a^2} \quad [10]$$

We have collapsed all the geometric terms except for the pit width variable (*a*) into the parameters A_o and B_o. This results in the following form for *A* and *B*:

$$A \sim P\left(A_o - \frac{2}{a^2}\right) \quad [11a]$$

$$A_o = \frac{1}{h^2} - \frac{1}{(h+d)^2} \quad [11b]$$

$$B \sim \frac{B_o}{a^2} \quad [12a]$$

$$B_o = \frac{w}{(h+d)} \quad [12b]$$

The best fit reveals parameters A_o=102 μm^{-2} and B_o=4.17×10^{-2}. Comparison with the parameters predicted from using equations 11b and 12b with the geometry dimensions for the chip show that the fit parameters A_o and B_o are both smaller by 64.4% than the calculated values. We introduce fitting parameters κ_1 and κ_2 which modify the current predictions for A_o and B_o. Since these experiments were conducted for a different slit height and pit depth than the original experiments by Reisner, κ_1 and κ_2 would be possible functions of these variables. The new fitting parameters would be implemented as follows:

$$A_o = \kappa_1\left(\frac{1}{h^2} - \frac{1}{(h+d)^2}\right) \quad [13a]$$

$$B_o = \kappa_2\left(\frac{w}{(h+d)^2}\right) \quad [13b]$$

A look at the dashed curve in figure 8 obtained from computation using the definitions of parameters A_o and B_o in equations 11b and 12b shows that qualitatively the theory works very well, but it seems to overestimate the average pit occupancy probabilities. However, at *a*=200nm it predicts something very counter-intuitive; the average pit occupancy probability drops drastically. If the nanopit is small compared to the persistence length *P* of the DNA molecule, it may be the case that it is simply energetically unfavourable for the molecule to occupy a nanopit. Introducing the fitting parameters κ_1 and κ_2 can eliminate this abrupt drop in occupancy probability, and seems to show that the excluded volume term (*B*) and the entropic parameter (*A*) exhibit a weaker dependence on slit height and pit depth than currently predicted.

CONCLUSION

We have demonstrated that the theory for predicting the occupancy states for molecule length variation of λ-DNA does not adequately show the sharp transitions that are observed in experiment; pit width variation, however, is in good qualitative agreement. We show that by calibrating the measurements of fluorescence intensity with a known molecule length, it is possible to histogram the average occupancy versus intensity data to discern between variably-sized DNA fragments. We demonstrate that a least-squares fit of the pit-width variation data seems to suggest that the geometric parameters A_o and B_o in current theory may have to be modified. To fit our experimental results to current theory, hypothesized pre-factors, κ_1 and κ_2, were introduced. Future work should be carried out to probe the regimes where counter-intuitive behaviour is predicted by the probability distributions for average pit occupancy (especially where pit widths are below 200nm).

ACKNOWLEDGEMENTS

I wish to thank Prof. Walter Reisner for his generous assistance and guidance throughout this project. Also, I wish thank Qikuan Zhou and André Brandão for their insightful and interesting discussions on how to tackle the lengthy programming for the data analysis, and Alex Klotz for his assistance in conducting the experiments. Finally, I wish to acknowledge NSERC and McGill University for the financial support provided to fund this re search.

REFERENCES

1. P. de Gennes, in *Scaling Concepts in Polymer Physics*. (Cornell Univ. Press, Ithaca, NY, 1979).
2. S. F. Edwards, in *Molcular Fluids*. (Gordon and Breach, London, 1976).
3. C. H. Reccius, John Thomas Mannion, Joshua David Cross, and H. G. Craighead, *Physics Review Letters* **95**, 268101 (2005).
4. W. Reisner *et al. Physics Review Letters* **99**, 058304 (2007).
5. A. Balducci, C.-C. Hsieh, and P. S. Doyle, *Physics Review Letters* **99**, 238102 (2007).
6. E. A. Strychalski, Stephen Levy, and H.G. Craighead, *Macromolecules* **41**, 7716 (2008).
7. W. Reisner, Niels B. Larsen, Henrik Flyvbjerg, Jonas O. Tegenfeldt, and Anders Kristensen, *PNAS* **106**, 79-84 (2009).
8. W. Reisner, *et al. PNAS* **107**, 13294-13299 (2010).
9. D. C. Sullivan, Tiba Aynechi, Vincent A. Voelz, and Irwin D. Kuntz, *Biophysical Journal* **85**, 174-190 (2003).
10 D. Stein, Frank H. J. van der Heyden, Wiepke J. A. Koopmans, and Cees Dekker, *PNAS* **103**, 15853-15858 (2006).
11 S. P. Robert Fisher, Ashley Walker, Erik Wolfart. http://homepages.inf.ed.ac.uk/rbf/HIPR2/log.htm. Accessed July 10th, 2010.